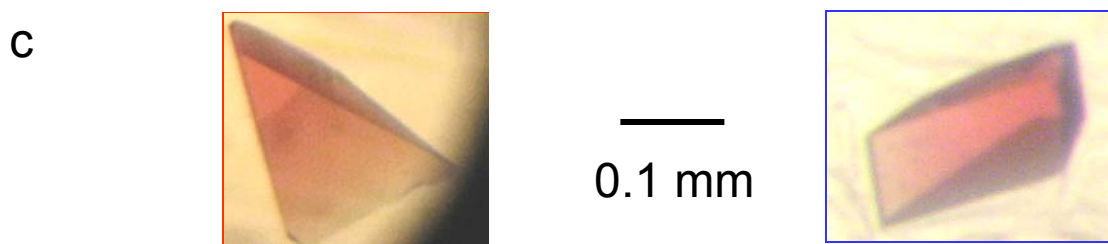
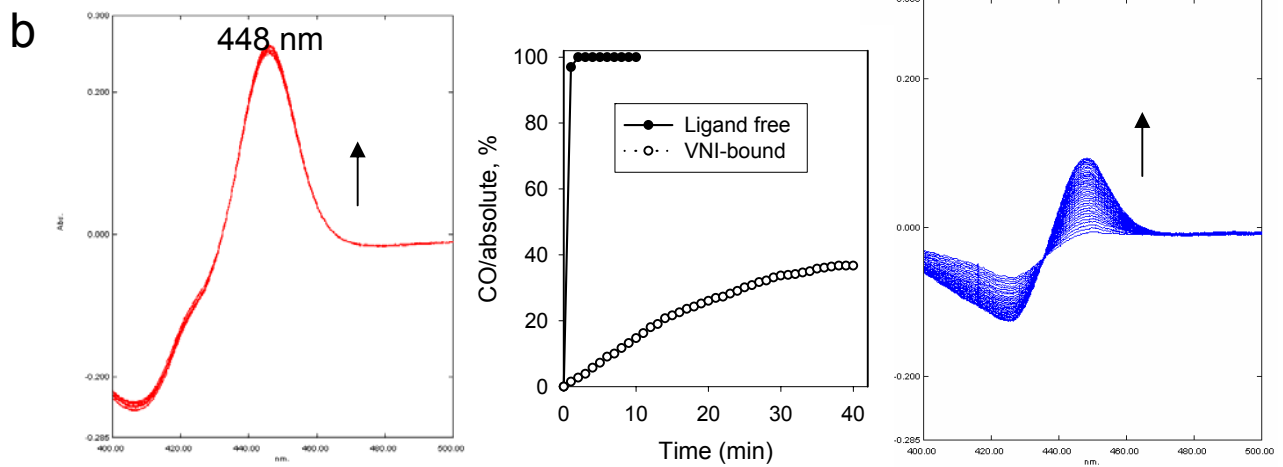
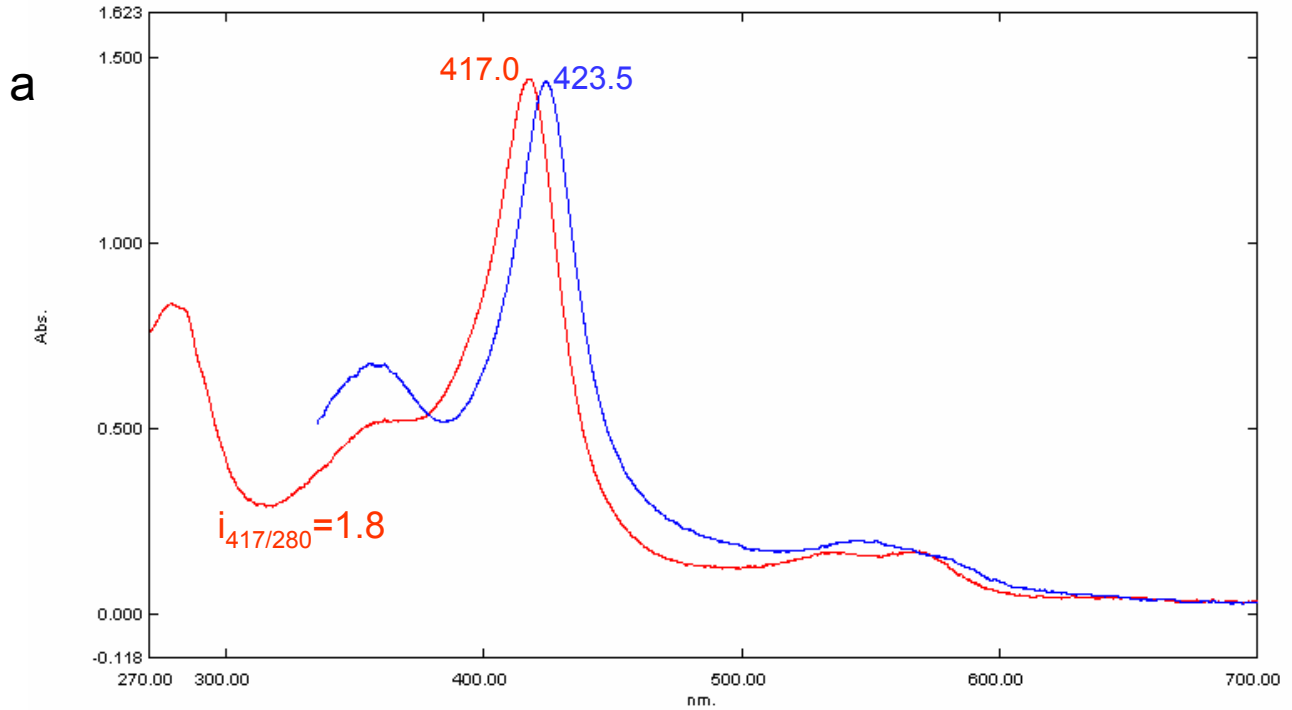
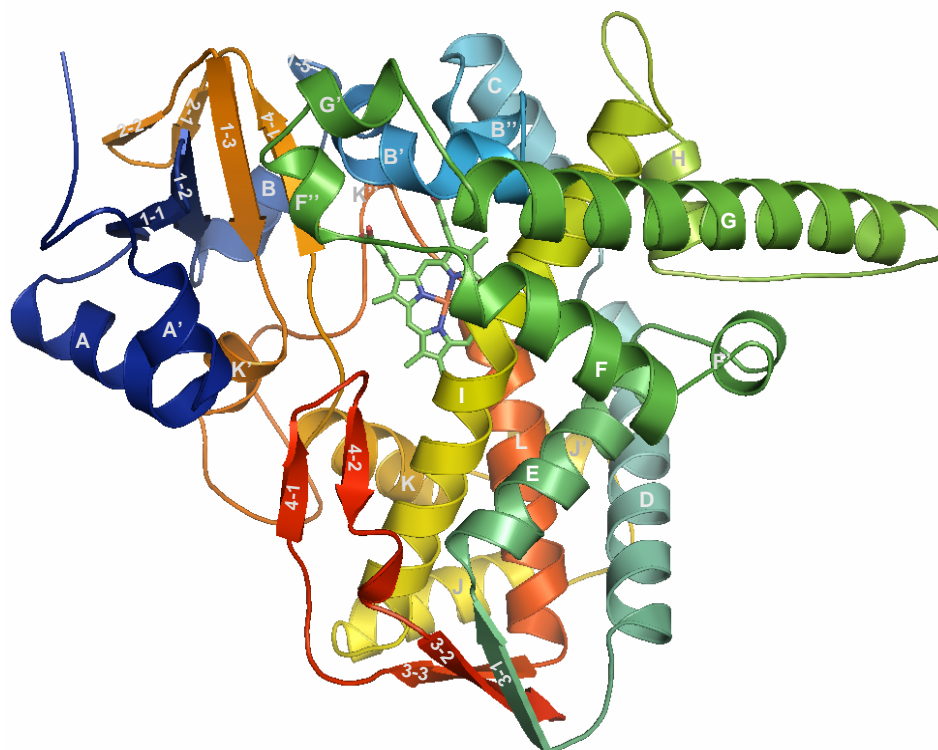


**Supplemental Figure S1.** The three-step 14DM reaction, each step requires two reducing equivalents from NADPH (transferred via the FAD and FMN cofactors of cytochrome P450 reductase), two protons and one molecular oxygen. Only  $R_1$  (H or  $\text{CH}_3$ ) and  $R_2$  (H or  $=\text{CH}$ ) vary in the 14DM substrates across the biological kingdoms. In the enzyme active center, the  $14\alpha$ -methyl group of the substrate is sequentially converted into the alcohol, then into the aldehyde derivative and then it is released as formic acid concomitantly with the introduction of the  $\Delta^{14-15}$ -double bond into the sterol core.



**Supplemental Figure S2. Ligand-free (left/red) and VNI-bound (right/blue) Tbb14DM. a.** Absolute absorbance; **b.** CO-difference spectra ( $\Delta t=1$  min) Time-course graph shows the rate and percentage of CO-complexes formation in ligand-free and VNI-bound state. **c.** Crystals.



**Supplemental Figure S3. A ribbon diagram showing the overall Tbb14DM structure. Distal view.** N-terminus (starting at G29) is colored in dark blue, and the C-terminus (ending at R476) is colored in red, full-length protein numbering. The 12 main helices are labeled from A to L; ten additional shorter helices between them are marked as (') and 12  $\beta$ -strands arranged in 4 bundles are labeled by structure succession (5 strands in bundle 1, 2 in bundle 2, 3 in bundle 3, and 2 in bundle 4). The heme is shown in stick representation.



T.b\_brucei

Sequence alignment of the first 100 amino acids of the protein across various species including T.b\_brucei, T.b\_gambiense, T.congolense, T.vivax, T.cruzi, L.infantum, L.amazonensis, L.major, L.braziliensis, C.albicans, Human, M.tuberculosis, and M.tuberculosis.

Sequence alignment of the first 100 amino acids with domain annotations: alpha A', alpha A, beta 1-1, beta 1-2, alpha B, beta 1-5, eta B', and alpha B'. Residue numbers 42-58 are shown.

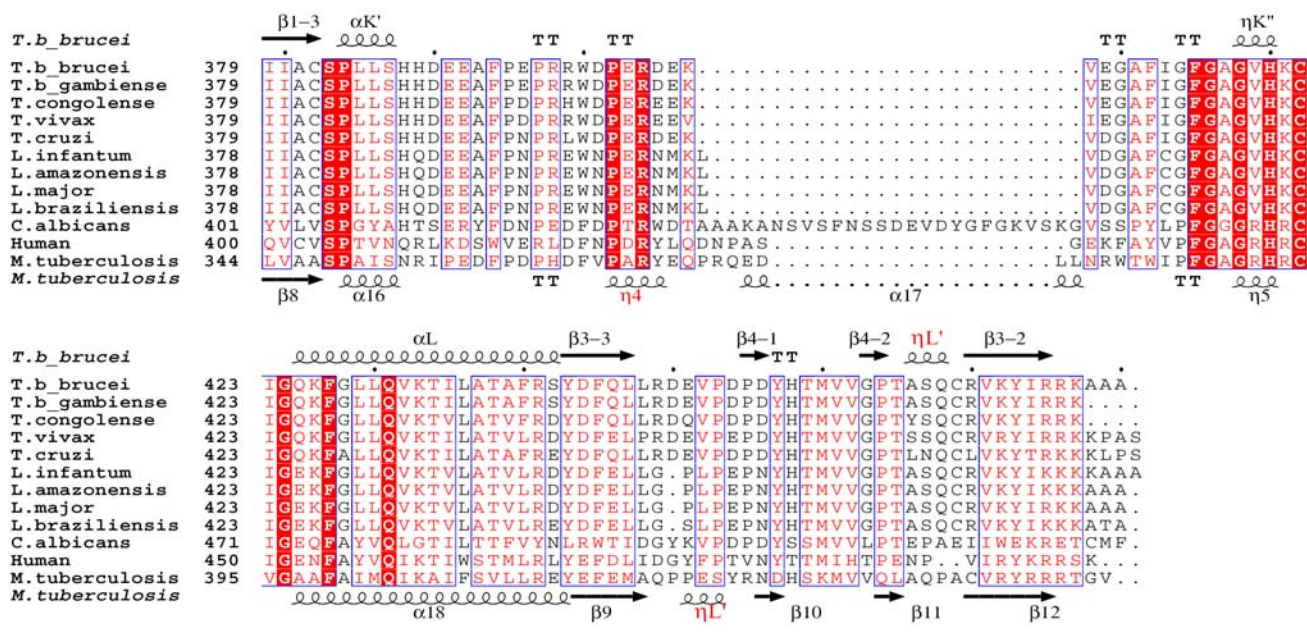
Sequence alignment of the first 100 amino acids with domain annotations: eta B', alpha C', alpha D, beta 3-1, and alpha E. Residue numbers 111-140 are shown.

Sequence alignment of the first 100 amino acids with domain annotations: alpha F', alpha F, eta F'', eta G', and alpha G. Residue numbers 176-203 are shown.

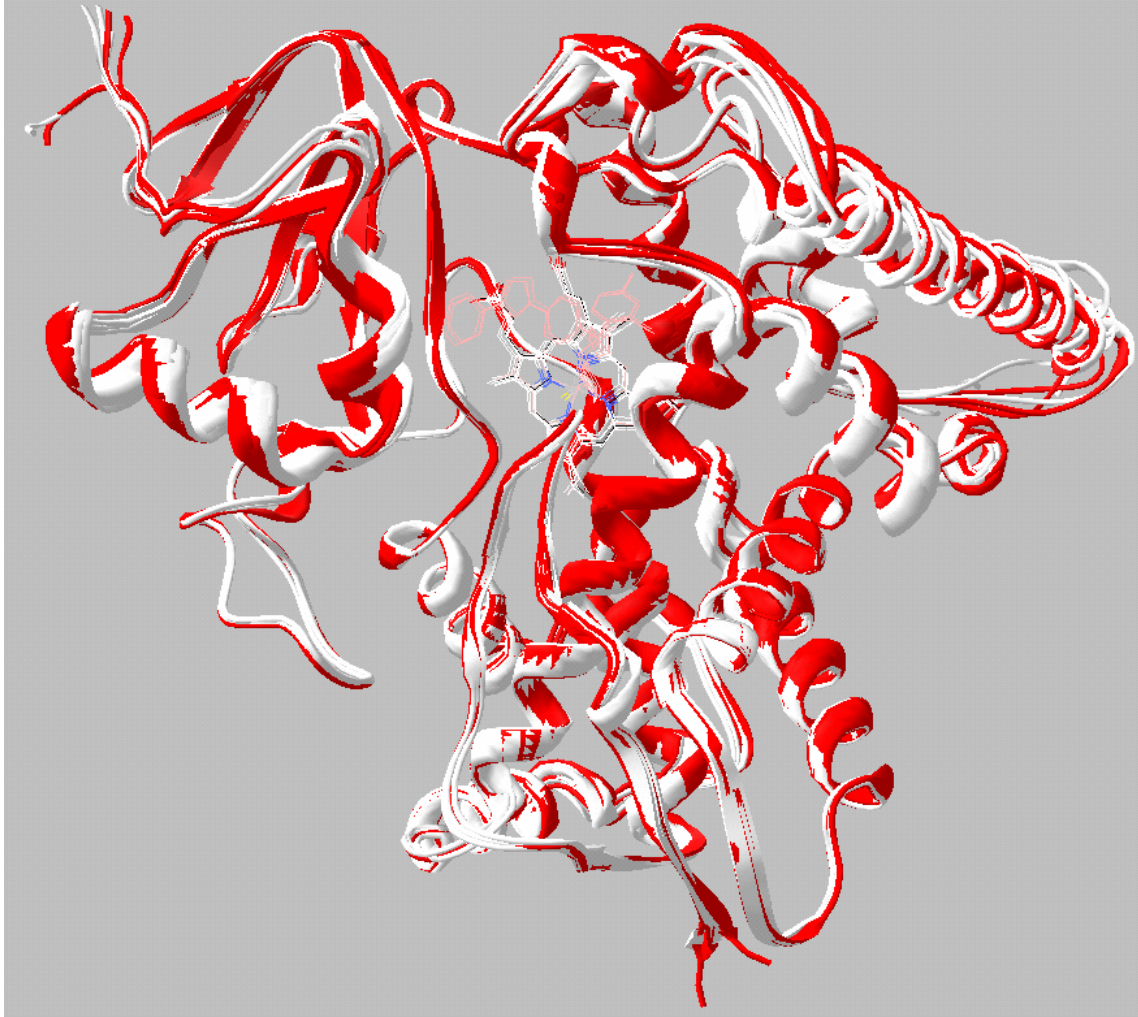
Sequence alignment of the first 100 amino acids with domain annotations: alpha H, alpha I, alpha J, alpha K, beta 1-4, beta 2-1, and beta 2-2. Residue numbers 246-280 are shown.

Sequence alignment of the first 100 amino acids with domain annotations: alpha J, alpha J', alpha K, beta 1-4, beta 2-1, and beta 2-2. Residue numbers 315-336 are shown.

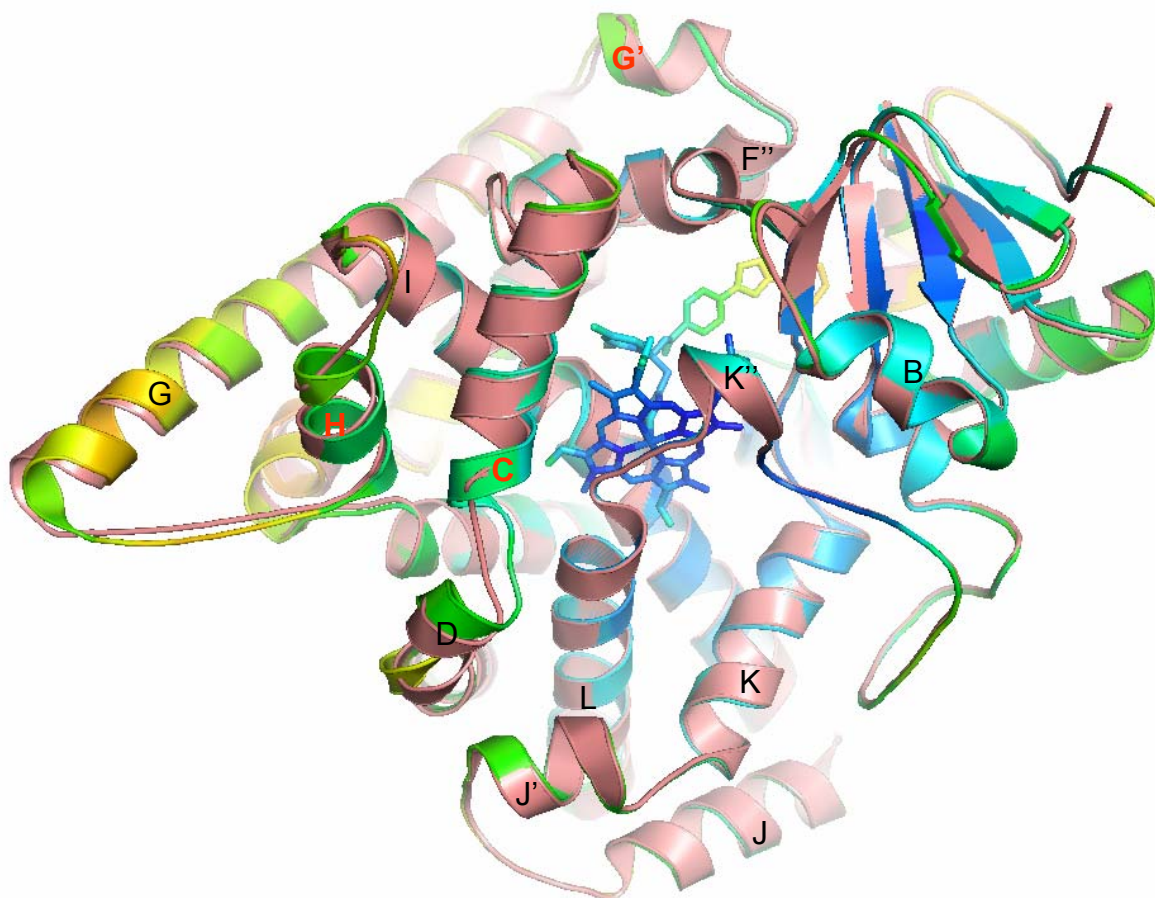




**Supplemental Figure S4. Sequence alignment of 14DMs from *Trypanosomatidae* (75% average amino acid sequence identity), *Candida albicans* (24% identity to *Tbb14DM*), human (27% identity) and *Mycobacterium tuberculosis* (27% identity). Secondary structure elements of 14DM from Tbb and Mt are shown at the top and the bottom, respectively. The P450-fold nomenclature is provided for Tbb14DM; differences in the secondary structure elements are indicated in red.**

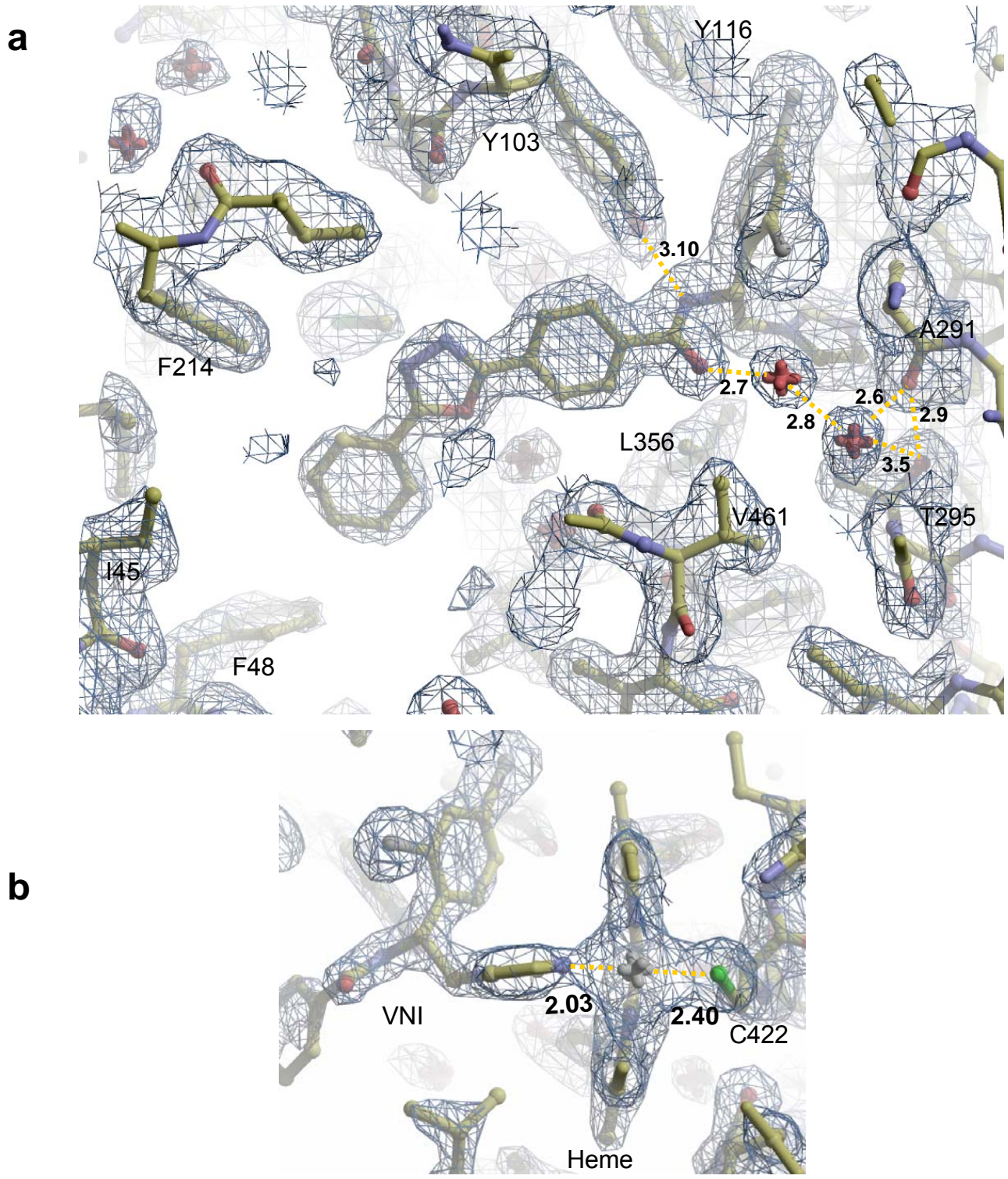


**Supplemental Figure S5. Superimposition of four molecules of ligand-free (white) and four molecules of VNI-bound (red) Tbb14DM (distal view).**



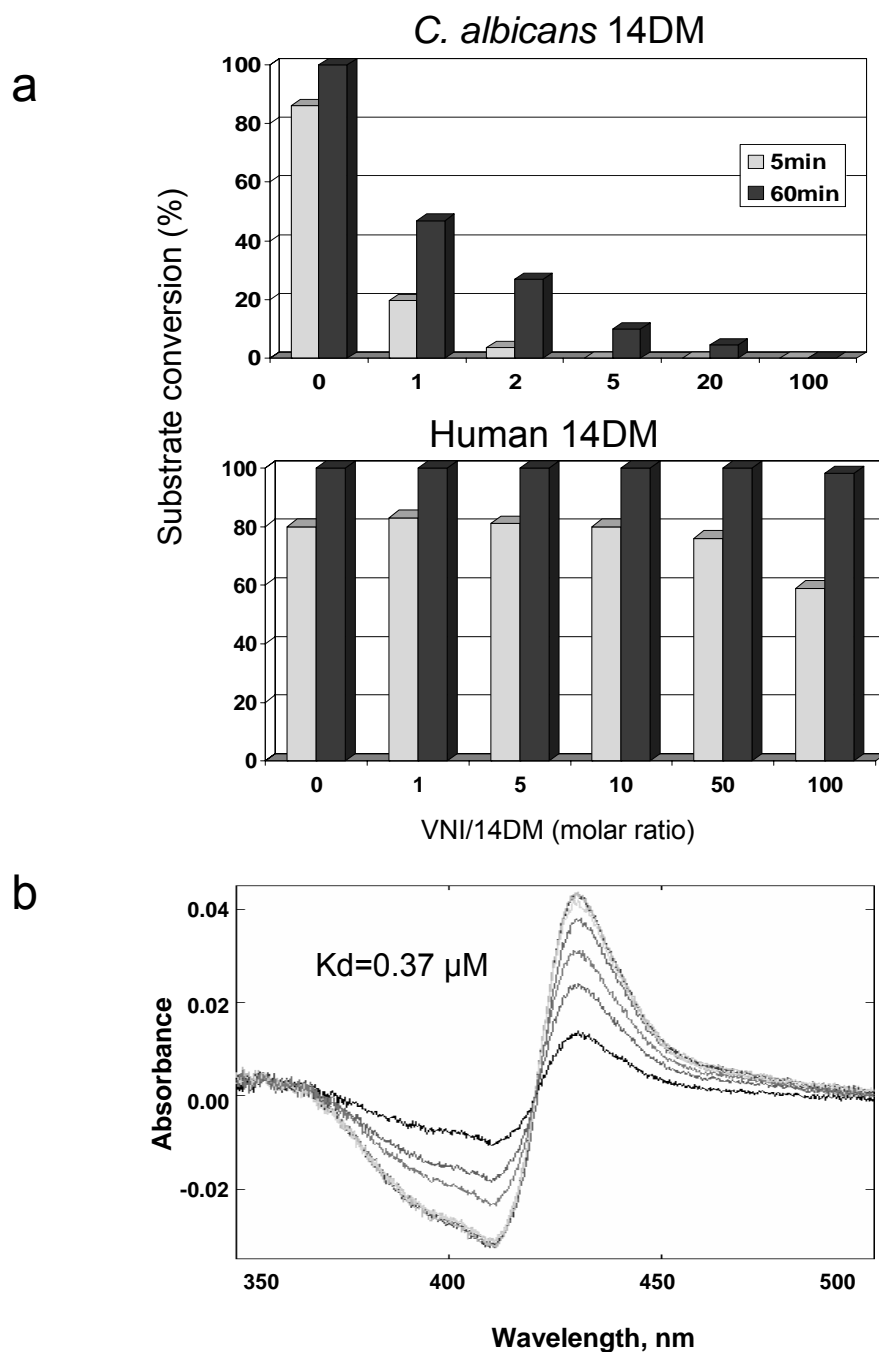
**Supplemental Figure S6. View of the superposed ligand-free and VNI-bound Tbb14DM structures from the proximal (opposite to Fig.2b) side.** Some shift toward the heme in the VNI-bound structure can be seen for helices C, D, H, J and the C-terminal part of helix G. Elongated secondary structure elements (helices C, H and G' in all four molecules) are marked in red near the places of their extensions. The tendency to form additional helix-like turns has been also observed for azole-bound drug-metabolizing CYP2B4 [1SUO and 2V0M] and for substrate-bound CYP46A1 [2q9f] and might indicate some additional molecule surface stabilization.



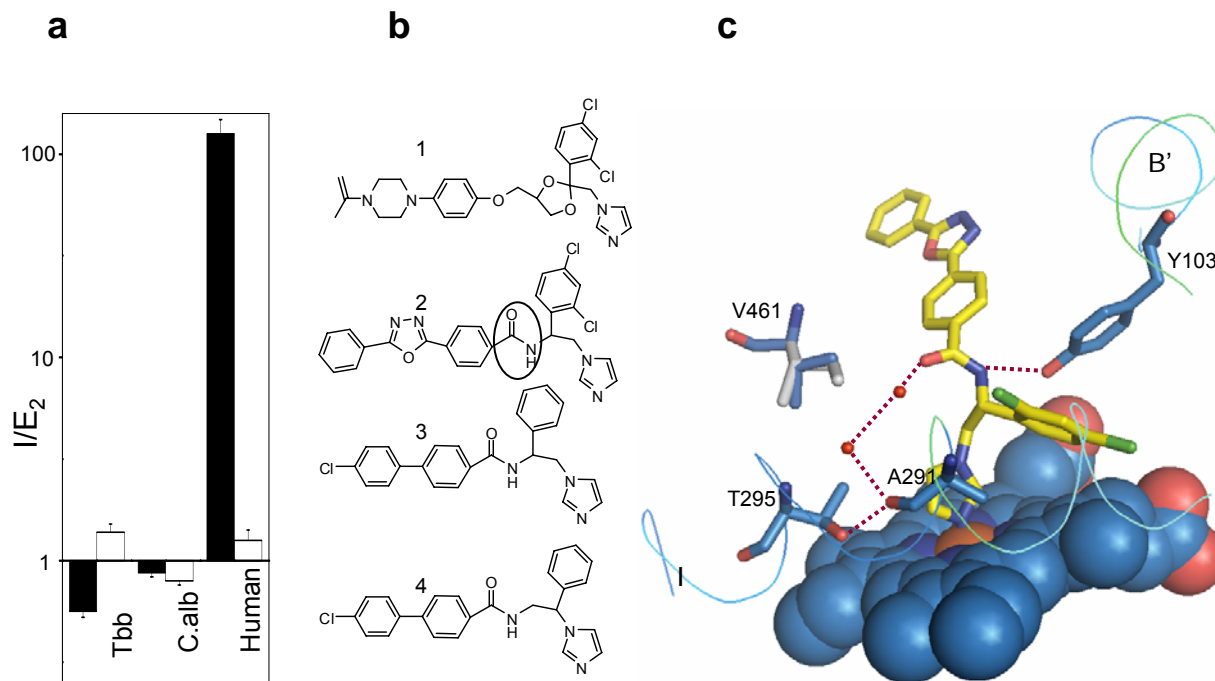


**Supplemental Figure S7. 2Fo-Fc electron density map for VNI in the active site of Tbb14DM contoured at 1  $\sigma$  (a) and 2.5  $\sigma$  (b). The bond distances ( $\text{\AA}$ ) are marked.**





**Supplemental Figure S8. a. Inhibition of *C. albicans* and human 14DM activity by VNI.** Enzyme concentration  $0.5 \mu\text{M}$ , substrate (lanosterol) concentration  $50 \mu\text{M}$ ,  $\text{SD} < 10\%$ . The other details of the reaction conditions are as described in (19). **b. Binding of VNI to human 14DM**, difference absorbance spectra. The human 14DM concentration  $1.7 \mu\text{M}$ ;  $1\text{mM}$  VNI solution in DMSO, titration range  $0.5\text{--}4 \mu\text{M}$ , titration step  $0.5 \mu\text{M}$



**Supplemental Figure S9. VNI amide group fragment as the most likely cause for its selectivity towards 14DM from pathogenic microbes.** **a.** Comparison of inhibitory effects of VNI (black bars) and clinical antifungal drug ketoconazole (white bars) on 14DMs from two pathogens, Tbb and *Candida albicans*, and from human.  $I/E_2$  represents the inhibitor/enzyme ratio that causes a two-fold decrease in the initial rate of reaction, log scale. **b.** Chemical structures of ketoconazole (1), VNI (2) and two VNI-scaffold derivatives: the  $\beta$ -phenyl azole SDZ285604 (3) with the inhibitory potency and antiparasitic effect in *Trypanosomatidae* comparable to VNI and the  $\alpha$ -phenyl azole SDZ285428 (4), a competitive, “short-term” inhibitor that binds with the same apparent  $K_d$  (<100 nM) but can be easily replaced in the enzyme active site by substrate (11). **c.** VNI-induced hydrogen bonding network between helices B' and I. V461 and its mutation to isoleucine (grey), corresponding to I488 in human 14DM, are shown. Heme is presented as spheres.

## Supplemental Table S1. Data collection and refinement statistics

	Ligand-free		Inhibitor-bound
Data collection	Native	Iron SAD (peak)	Native
Wavelength, Å	0.980	1.7389	0.980
Space group	P1	P1	P1
Cell dimensions			
a, b, c, Å	59.8, 79.9, 117.1	59.7, 79.9, 116.7	60.1, 79.1, 116.0
$\alpha$ , $\beta$ , $\gamma$ , °	74.2, 81.6, 68.5	74.4, 81.1, 68.5	74.7, 79.1, 68.6
Number of molecules per asymmetric unit	4	4	4
Resolution, Å	30-1.89 (1.94-1.89)*	50-2.60 (2.69-2.60)	50-1.87 (1.9-1.87)
R <sub>merge</sub>	0.060 (0.470)	0.077 (0.536)	0.050 (0.603)
I/ $\sigma$ (I)	18.5 (3.1)	44.5 (3.4)	28 (1.8)
Completeness (%)	97.8 (96.7)	96.8 (95.2)	96.99 (91.7)
Redundancy	4.0 (3.8)	7.8 (7.7)	3.9 (3.5)
Refinement			
Resolution, Å	28.7-1.89		37.5-1.87
Number of reflections	142,726		144,527
R <sub>work</sub> / R <sub>free</sub>	0.195/ 0.234		0.189/0.238
Average B-factors			
protein	36		35
heme/inhibitor	22		23/32
water	40		38
Rms deviations			
Bond lengths, Å	0.026		0.017
Bond angles, °	1.894		1.549
C $\alpha$ positions between 4 molecules, Å	0.51		0.54

\*Values in parenthesis are for highest-resolution shell.